Green synthesis of Copper oxide and Cobalt oxide nanoparticles using Spinacia Oleracea leaf extract

Authors: Yameen Ahmed [1*], Jamshaid Hussain [1], Sohaib Asif [2]

Affiliations: [1] Hazara University Mansehra, KPK
[2] School of Computer Science, COMSATS University, Pakistan

*Corresponding Author: yameenwazir@yahoo.com

Abstract
The investigation aims at the synthesis of copper oxide and cobalt oxide nanoparticles using Spinacia Oleracea leaf extract. The Spinacia Oleracea leaf extract behaves as a reducing agent in the nanoparticle synthesis. Plant extract was first prepared and then treated with copper and cobalt salt solutions to get the precipitate. The salt solutions used for this purpose are copper sulphate pentahydrate ($CuSO_4.5H_2O$) and cobalt chloride hexahydrate ($CoCl_2.6H_2O$). The UV-Vis, XRD, EDX and SEM techniques are used to find optical, structural and morphological properties of copper oxide and cobalt oxide nanoparticles. The average crystallite size of copper oxide nanoparticles is 44 nm and have a hexapod structure. The UV absorption peaks are at 326 nm and 506 nm for copper oxide and cobalt oxide nanoparticles.

Keywords: Nanoparticles; cobalt oxide; copper oxide; green synthesis.

Introduction
In the nanoscience applications, nanoparticles with a size of less than 100 nm are being widely used [1]. Metal oxide and metal nanoparticles (NPs) are emerging candidates in the field of nanotechnology and nanoscience. Depending on their shape and size, these nanoparticles with optical, electrical and physical properties play a vital role. They have a large number of applications, such as antioxidants, catalysis, sensors, antibacterial, etc. Oxides of metal nanoparticles such as, CoO, ZnO, TiO_2, SnO_2 and CuO, have been studied for their biomedical and environmental applications [2]. For the synthesis of nanoparticles, various chemical and physical methods have been used which includes; high-temp solution phase, thermal decomposition, hydro-thermal micro emulsion and reduction etc. [3]. However, green synthesis of nanoparticles is considered as a significant branch of nanotechnology [4, 5]. This method is cost effective and eco-friendly as compared to the conventional synthesis methods, where chemical additives, high temperature pressure and energy are used [6]. Therefore, it is necessary to develop and use safe methods which must be low cost, efficient, and non-hazardous and environment friendly. Due to this reason, many researchers adopted green synthesis method to fabricate nanoparticles [7]. Materials which are derived from plants are used to prepare nanoparticles and is also the best alternative to chemical and physical method. Plant extracts contain bio-active compounds like flavonoids, saponin, phenolic acid and tannins [8]. These bioactive compounds are good chelation agents and can donate hydrogen and quench singlet oxygen. Due to their redox activities green synthesis of NPs is more suitable than the physio-chemical techniques. Plant extracts can be processed via easy protocols and are easy to handle and non-toxic [9, 10].

Copper oxide nanoparticles exhibit high potentiality in the metal oxide NPs owing to its antimicrobial, catalytic, optical and low-cost properties. Copper oxide NPs have a bandgap ranging from 1.35-3.5 eV. Due to their suitable bandgap, easy availability, low toxicity and surface synthesis among different semiconductor photocatalysts [11]. Copper oxide NPs gain attention due to its good oxygen adsorption capability and large surface area and considered a promising candidate with good photocatalytic activity [12]. Copper oxide is a widely studied semiconductor of II-VI group and is a p type semiconductor. Because to its good optical properties which allows stable emission at room temperature, it is used in various applications such as photonic and field emission devices and sensors [13]. Copper oxide NPs can

be used as magnetic storage media, optical switch and gas switch due to its photochemical and photoconductive properties [14].
Cobalt oxide NPs are used in wide range of applications owing to their oxidation as well as high resistance to corrosion [15]. It is a p-type anti-ferromagnetic semiconductor. It is a multifunctional material with many applications such as energy storage materials, anode in Li-ion batteries, dyes and pigments, sensors and heterogeneous catalysis [16]. Apart from the green synthesis, different chemical and physical techniques were used to synthesis cobalt oxide nanoparticles such as solution combustion method, microwave process, thermal decomposition of sol gel, hydrothermal reaction etc. [17].
Many researchers have reported the green synthesis of copper oxide nanoparticles using different plant extract such as Lemongrass [18], Madhuca longifolia [19], Aspergillus fumigates [20], Nerium oleander [21], Bifurcaria bifurcate [22], Euphorbiaesula [23], and Albizia lebbeck [24]. Arunkumar et al. [11] showed the degradation of MB dye at 94% on irradiation by using the copper oxide nanoparticles synthesized via the Lantana camara leaf extract. Sathiyayimal et al [25] showed 93% degradation of MB dye in about 100 min by using the copper oxide nanoparticles synthesized via Sidaacuta leaf extract.
Cobalt oxide nanoparticles using plant extract has been investigated in various research articles such as Diallo et al. [26] discovered the bio reduction ability of the Aspalathus linearis leaf extract for cobalt oxide NPs synthesis. Bibi et al. [27] synthesized cobalt oxide NPs using Punica granatum peel extract from cobalt nitrate hexahydrate. Dubey et al. synthesized cobalt oxide nanoparticles using Calotropis procera leaf extract [28].

In our work, we synthesized copper oxide and cobalt oxide nanoparticles using an environmental friendly method. Spinacia Oleracea leaf extract was used for the green synthesis of nanoparticles.

Materials and Methods

Preparation of Leaf Extract

For the preparation of leaf extract, fresh leaves of Spinacia Oleracea (Spinach) were collected from the local field of Dhodial, Mansehra by wearing gloves. These leaves were then washed 3 times with tap water to remove dust from it, washed it again 3 times with distilled water and placed them on a clean aluminum foil to dry for about 3 hours. After that, the leaves were cut into small pieces with the help of scissors. Then weighed 10 g of cut leaves with the help of electric weight balance, put these 10 g of leaves in 100 ml deionized water and placed a magnetic bar into it and sealed the opening of the beaker with aluminum foil to protect it from the dust present in the surroundings, then placed the beaker on magnetic stirrer for 50 minutes at 70^{o}C. We saw that the color of the water changed to yellow as shown in figure 1 (a). The beaker is removed from the magnetic stirrer and placed it on a table for about 20 min and let it cooled. When the water got cooled, it is filtered with the help of Whatmann filter paper in a conical flask. The flask is then sealed with aluminum foil. The flow chart for the preparation of leaf extract is shown in figure 1 (d).

Synthesis of Copper Oxide Nanoparticles

Placed the copper sulphate pentahydrate solution on the magnetic stirrer and put a magnetic bead in the beaker. Details of salt concentration is given in table 1. After about 20 minutes of heating, 10 ml of Spinacia Oleracea leaf extract was added drop wise in the solution using a burette. About 10 minutes after addition of leaf extract, the color the solution changed from light blue to green as shown in figure 1 (b). The temperature at that time was noted to be 70^{o}C. Then, removed the solution from the magnetic stirrer and placed it on a safe place to let it cool, also covered the beaker with aluminum foil to protect it from dust particles. Next day the cooled solution then put into three test tubes, these test tubes were then placed into the centrifuge for 20 minutes and set the centrifuge to 4500 rotations per minute. One test tube is then used for UV and the other two were saved for further characterizations. Details of synthesis is given in table 2.

Synthesis of Cobalt Oxide Nanoparticles

Placed the cobalt chloride hexahydrate solution on the magnetic stirrer and put the magnetic bead in the beaker. Details of salt concentration is given in table 1.After about 15 minutes of heating, 15 ml of Spinacia Oleracea leaf extract was added drop wise in the solution using a burette. About 10 minutes after the addition of leaf extract the color the solution changed from light pink to reddish as shown in figure 1 (c). The temperature at that time was noted to be 70ºC. Then, removed the solution from the magnetic stirrer and placed it on a safe place to let it cool, also covered the beaker with aluminum foil to protect it from dust particles. Next day the cooled solution then put into three test tubes, these test tubes were then placed into the centrifuge for 20 minutes and set the centrifuge to 4500 rotations per minute. One test tube is then used for UV and the other two were saved for further characterizations. Details of synthesis is given in table 2.

Table 1 Details of salt concentrations

Salts	Distilled water (ml)	Salt Concentration (M)	Salt concentration (g)
Copper Sulphate Pentahydrate ($CuSO_4.5H_2O$)	100	0.12	3
Cobalt Chloride Hexahydrate ($CoCl_2.6H_2O$)	100	0.106	2.5

Table 2 Details about the synthesis of nanoparticles

Salt	Salt concentrations (ml)	Leaf extract concentrations (ml)	Time taken for heating (min)	Temperature (˚C)	Time taken for centrifuge (min)
($CuSO_4.5H_2O$)	0.12	10	30	70	20
($CoCl_2.6H_2O$)	0.106	15	30	70	20

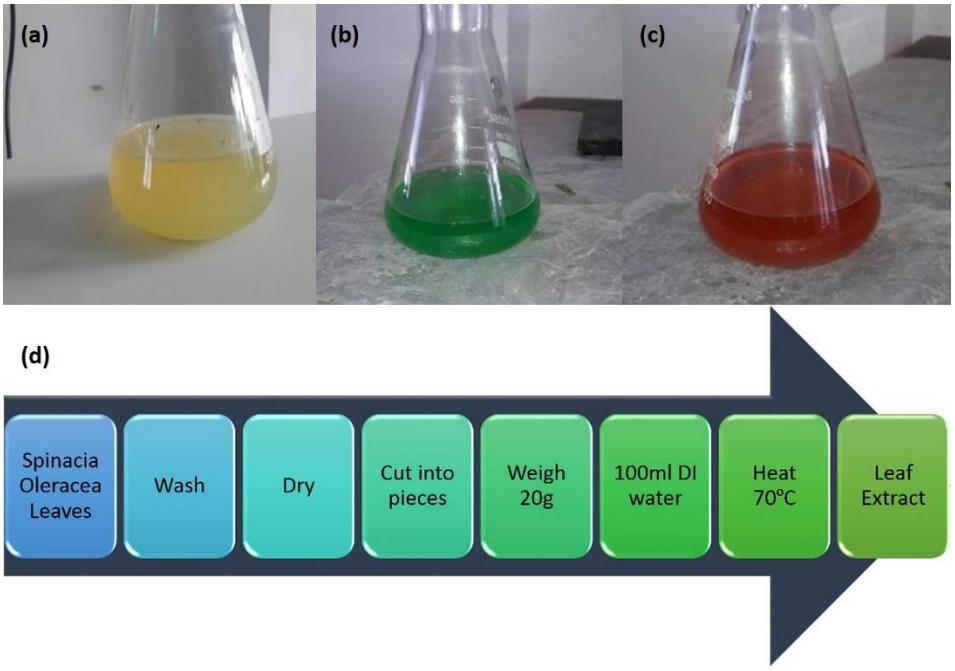

Figure 1 (a) leaf extract, (b) Copper oxide nanoparticles solution, (c) Cobalt oxide nanoparticles solution, (d) Flow chart for the preparation of leaf extract.

RESULTs AND DISCUSSION

The absorbance peak for biosynthesized Copper oxide nanoparticles from Spinacia Oleracea extract was at 326 nm indicating the formation of copper oxide nanoparticles from Copper Sulphate Pentahydrate. To analyze the optical properties of extracted copper oxide NPs, the optical absorption spectra was used. From this spectrum the type of electronic transition and the band gap of the material were determined [29]. When a material absorbs photon of energy greater than the energy band gap, an electron is transported to the conduction band (CB) from the valence band (VB), an immediate rise in the absorbance of the semiconductor to the wavelength occurs corresponding to the energy of the band gap. The relationship of the incident photon to the absorption coefficient depends on the electronic transition type. The transition is direct if the momentum is conserved and it is indirect if the momentum is not conserved. Figure 2 (a) shows the absorption spectrum of copper oxide nanoparticles. The UV-Vis spectrum showed the absorption peak at 326 nm and the cut off wavelength at 400 nm. The reported material is a direct band gap semiconductor material. According to the literature, the absorption peak of copper oxide nanoparticles ranges from 250-300 nm, but in our work the absorption peak is at 326 nm. The higher value of absorption peak is due to the formation of some other metastable and stable copper oxide NPs. The energy band gap was calculated from the equation $E_g = hc/\lambda$. Where λ is the cut-off wavelength, $c = 3 \times 10^8$ m/s is the speed of the light and $h = 4.13566 \times 10^{15}$ eV is the Plank's constant. The energy bandgap comes out to be 3.1 eV. The cut-off wavelength was obtained by extrapolating the line to the base, where α is zero. As compared to the bulk value (3.25 eV), there is a slight blue shift in the band gap (3.1 eV) [29] which is due to the quantum confinement effect [30].

The absorbance peak for biosynthesized Cobalt oxide NPs from Spinacia Oleracea extract was at 509 nm indicating the formation of cobalt oxide nanoparticles from cobalt chloride hexahydrate. The UV-Vis spectrum of cobalt oxide NPs showed the absorption peak at 509 nm as shown in figure 2 (b). This absorption band can be attributed to the plasma resonance absorption of the cobalt oxide nanoparticles. Cobalt oxide nanoparticles show a plasmon absorption band in between 350-550 nm which is its distinguishing feature [31]. The formation of non-oxide cobalt NPs might be the reason of the strong surface plasmon. The leaf extract of Spinacia Oleracea performs as a reducing cum surface capping agent that can be attributed to the synthesis of cobalt oxide NPs. In the presence of Spinacia Oleracea leaf extract, cobalt oxide nanoparticles were formed from the reduction of cobalt chloride hexahydrate, which acts as a capping, stabilizing and reducing agent [32]. The energy band gap was calculated from the equation $E_g = hc/\lambda$. Where λ is the cut-off wavelength, $c = 3 \times 10^8$ m/s is the speed of the light and $h = 4.13566 \times 10^{15}$ eV is the Plank's constant. The energy bandgap comes out to be 2.15 eV. The cut-off wavelength (575 nm) was obtained by extrapolating the line to the base, where α is zero.

The XRD spectrum (Fig. 2 (c)) reveals the diffraction peaks at different angles. XRD diffraction peaks at 24.406° and 25.978° corresponds to the planes (202) and (101) of Monoclinic CuO. The peak at 29.775° corresponds to the plane (110) of Cubic Cu_2O. The peak at 36.197°corresponds to the plane (004) of Tetragonal Cu_4O_3. The peaks at 18.283°, 18.553°, 20.03°, 27.93°, 29.543°, 31.653°, 44.656°, 55.071°, 57.823° corresponds to the planes (200), (103), (022), (301), (204), (153), (008), (056), (525) of Orthorhombic $Cu_{64}O$. The highest peak is detected at 2θ = 25.978° that matches to the diffraction of the CuO NPs having monoclinic structure. In our work, in addition to the stable oxides, i.e., CuO and Cu_2O, some other metastable oxides of copper such as Cu_4O_3, Cu_8O, and $Cu_{64}O$ have also been reported. These oxides are formed in the early stages of copper oxidation. These copper oxides are also found in pure copper powder which is commercially available. The sub-oxide $Cu_{64}O$ is formed when a very low amount of O atom mixed with Cu lattice with a ratio of 64:1 of Cu to O.

The crystallite size of the NPs were calculated by Debye-Scherer equation.

$$D = (0.9\lambda) / \beta \cos\theta$$

Where λ is the X-rays wavelength (Cu kα = 1.54604 Å), β is the full width half maximum value in radians, θ is the diffraction angle. The average size of copper oxide nanoparticles calculated by Scherer equation is 44 nm as shown in table 3.

Table 3 Details of size estimation, Bragg's angle and miller indices obtained from XRD

Degree°	(hkl)	FWHM	Size (nm)	Average Size (nm)
24.406	202	0.236	34	44
25.978	101	0.177	46	
29.778	110	0.472	17	
36.197	004	0.197	42	
18.283	200	0.098	82	
18.553	103	0.098	82	
20.03	022	0.118	68	
27.93	301	0.197	42	
29.543	204	0.157	52	
31.65	153	0.197	45	
44.65	008	0.394	22	
55.071	056	0.472	19	
57.823	525	0.394	23	

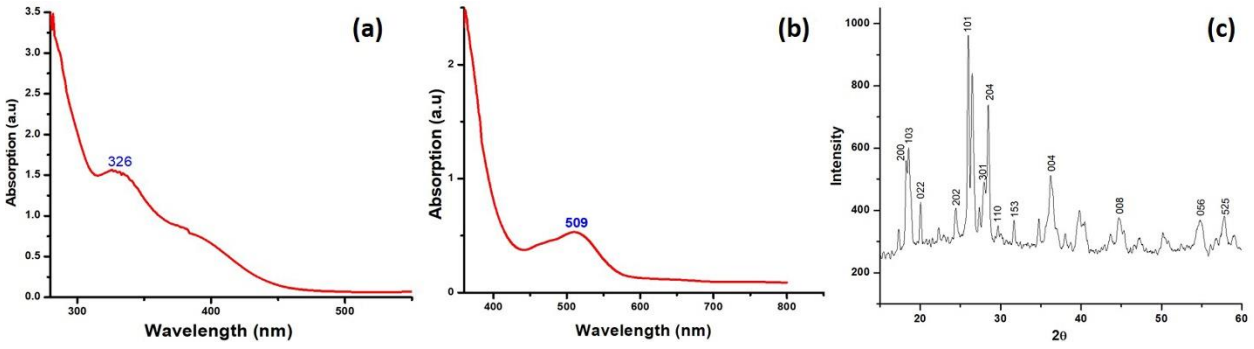

Figure 2 UV-Vis spectroscopy of (a) Copper oxide nanoparticles, and (b) Cobalt oxide nanoparticles, (c) XRD graph of copper oxide nanoparticles

Energy dispersive X-Ray (EDX) is used to study the elemental composition of the sample. Elements which are present in a sample can be identified by the released X-rays because every element has its own characteristic X-Ray. Using the EDX spectroscopy, Figure 3 (a, b) confirmed the presence of copper oxide and cobalt oxide nanoparticles. Generally typical absorption peaks of copper oxide nanoparticles are nearly at 0.5 keV and 8 keV as shown in figure 3 (a), while the typical absorption peaks of cobalt oxide nanoparticles are nearly at 0.8 keV, 6.9 keV and 7.6 keV as shown in figure 3 (b).

Scanning electron microscopy (SEM) is a characterization tool which provides the advance understanding of the morphology, shape and size of the nanoparticles. The copper oxide nanoparticles may have different shapes such as cubic, octahedral and hexapod. Figure 3 (c) shows the SEM image of synthesized hexapod copper oxide (Cu_2O) nanoparticles. Figure 3 (d, e) shows the SEM images of cobalt oxide nanoparticles, it is clear from the picture that the particles are agglomerated and spherical in shape. Compounds present in the extract and the nature of extract are main factors of agglomerations in the nanoparticles [33]. Large size nanoparticles form due to the attraction and reactivity of the functional groups. The synthesized particles have different biological compounds as coatings, these compounds have surface hydroxyl groups. Among these agents, intermolecular hydrogen bonding is present due to which the NPs appeared agglomerated.

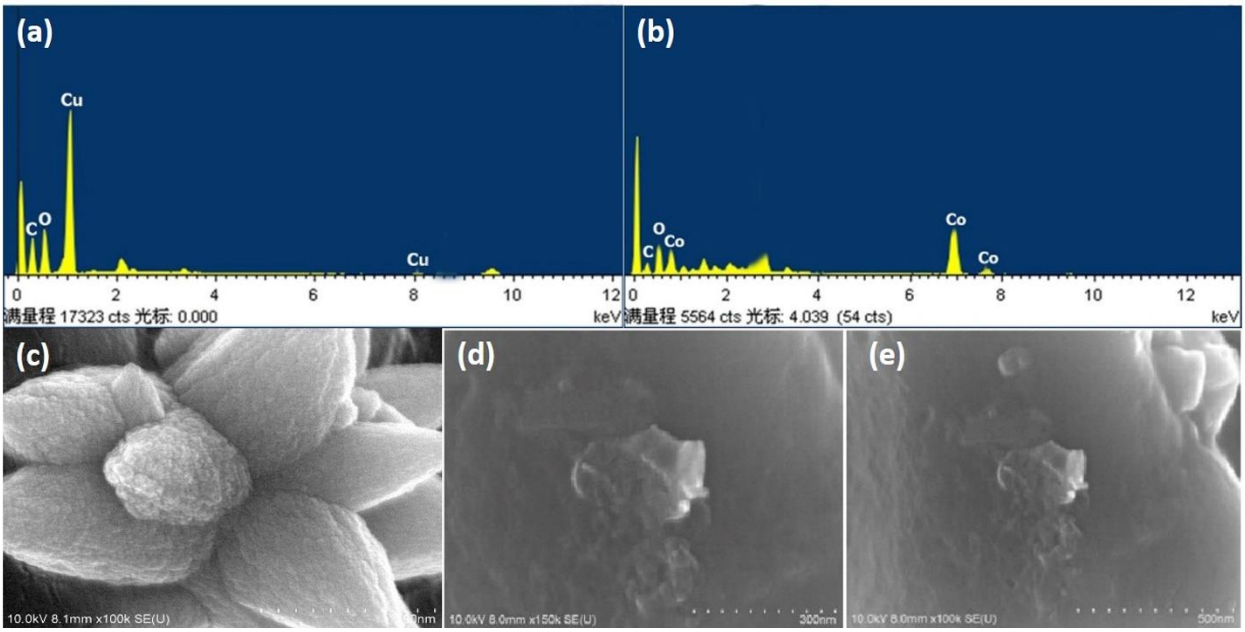

Figure 3 (a, b) EDX images of copper oxide nanoparticles and cobalt oxide nanoparticles. (c, d, e) SEM images of copper oxide nanoparticles and cobalt oxide nanoparticles

CONCLUSION

Copper oxide and cobalt oxide nanoparticles can be fabricated using reduction technique which is cheaper, environmental friendly and best comparing to other conventional techniques. In summary, we have established a facile green method to synthesize low cost copper oxide and cobalt oxide NPs by using Spinacia Oleracea leaf extract as both the capping and reducing agent. The synthesized NPs were examined by various techniques such as UV-Vis, XRD, EDX and SEM. These techniques confirmed the successful synthesis of copper oxide and cobalt oxide NPs. As we did not use any toxic material in the whole process, so it can be used in biomedical applications.

References

1. Linic, S., et al., *Photochemical transformations on plasmonic metal nanoparticles.* Nature materials, 2015. **14**(6): p. 567-576.
2. Muthuvel, A., M. Jothibas, and C. Manoharan, *Effect of chemically synthesis compared to biosynthesized ZnO-NPs using Solanum nigrum leaf extract and their photocatalytic, antibacterial and in-vitro antioxidant activity.* Journal of Environmental Chemical Engineering, 2020. **8**(2): p. 103705.
3. Remya, V., et al., *Silver nanoparticles green synthesis: a mini review.* Chemistry International, 2017. **3**(2): p. 165-171.
4. Patra, J.K., Y. Kwon, and K.-H. Baek, *Green biosynthesis of gold nanoparticles by onion peel extract: Synthesis, characterization and biological activities.* Advanced Powder Technology, 2016. **27**(5): p. 2204-2213.
5. Phukan, A., R.P. Bhattacharjee, and D.K. Dutta, *Stabilization of SnO2 nanoparticles into the nanopores of modified Montmorillonite and their antibacterial activity.* Advanced Powder Technology, 2017. **28**(1): p. 139-145.
6. Raveendran, P., J. Fu, and S.L. Wallen, *Completely "green" synthesis and stabilization of metal nanoparticles.* Journal of the American Chemical Society, 2003. **125**(46): p. 13940-13941.
7. Fazlzadeh, M., et al., *A novel green synthesis of zero valent iron nanoparticles (NZVI) using three plant extracts and their efficient application for removal of Cr (VI) from aqueous solutions.* Advanced Powder Technology, 2017. **28**(1): p. 122-130.

8. Asif, M., *7Antivral and antiparasitic activities of various substituted triazole derivatives: A mini review.* Chemistry International, 2015. **1**(2): p. 71-80.
9. Benouis, K., *Phytochemicals and bioactive compounds of pulses and their impact on health.* Chemistry International, 2017. **3**(3): p. 224-229.
10. Hailu, Y.M., et al., *Composition of essential oil and antioxidant activity of Khat (Catha edulis Forsk), Ethiopia.* Chem. Int, 2017. **3**: p. 25.
11. Arunkumar, B., S.J. Jeyakumar, and M. Jothibas, *A sol-gel approach to the synthesis of CuO nanoparticles using Lantana camara leaf extract and their photo catalytic activity.* Optik, 2019. **183**: p. 698-705.
12. Vinothkumar, P., et al., *Effect of reaction time on structural, morphological, optical and photocatalytic properties of copper oxide (CuO) nanostructures.* Journal of Materials Science: Materials in Electronics, 2019. **30**(6): p. 6249-6262.
13. Debbichi, L., et al., *Vibrational properties of CuO and Cu4O3 from first-principles calculations, and Raman and infrared spectroscopy.* The Journal of Physical Chemistry C, 2012. **116**(18): p. 10232-10237.
14. Chiang, C.-Y., et al., *Copper oxide nanoparticle made by flame spray pyrolysis for photoelectrochemical water splitting–Part II. Photoelectrochemical study.* International journal of hydrogen energy, 2011. **36**(24): p. 15519-15526.
15. Chen, M., J. Liu, and S. Sun, *One-step synthesis of FePt nanoparticles with tunable size.* Journal of the American Chemical Society, 2004. **126**(27): p. 8394-8395.
16. Kaviyarasu, K., et al., *Synthesis and characterization studies of NiO nanorods for enhancing solar cell efficiency using photon upconversion materials.* Ceramics International, 2016. **42**(7): p. 8385-8394.
17. Dong, C., et al., *Hydrothermal synthesis of Co3O4 nanorods on nickel foil.* Materials Letters, 2014. **123**: p. 187-190.
18. Le Tu, H., *Biosynthesis, characterization and photocatalytic activity of copper/copper oxide nanoparticles produced using aqueous extract of lemongrass leaf.* Composite Materials, 2019. **3**(1): p. 30-35.
19. Das, P., et al., *Madhuca longifolia plant mediated green synthesis of cupric oxide nanoparticles: a promising environmentally sustainable material for waste water treatment and efficient antibacterial agent.* Journal of Photochemistry and Photobiology B: Biology, 2018. **189**: p. 66-73.
20. Ghareib, M., et al., *BIOSYNTHESIS OF COPPER OXIDE NANOPARTICLES USING THE PREFORMED BIOMASS OF ASPERGILLUS FUMIGATUS AND THEIR ANTIBACTERIAL AND PHOTOCATALYTIC ACTIVITIES.* Digest Journal of Nanomaterials & Biostructures (DJNB), 2019. **14**(2).
21. Sebeia, N., M. Jabli, and A. Ghith, *Biological synthesis of copper nanoparticles, using Nerium oleander leaves extract: characterization and study of their interaction with organic dyes.* Inorganic Chemistry Communications, 2019. **105**: p. 36-46.
22. Abboud, Y., et al., *Biosynthesis, characterization and antimicrobial activity of copper oxide nanoparticles (CONPs) produced using brown alga extract (Bifurcaria bifurcata).* Applied Nanoscience, 2014. **4**(5): p. 571-576.
23. Nasrollahzadeh, M., S.M. Sajadi, and M. Khalaj, *Green synthesis of copper nanoparticles using aqueous extract of the leaves of Euphorbia esula L and their catalytic activity for ligand-free Ullmann-coupling reaction and reduction of 4-nitrophenol.* RSC Advances, 2014. **4**(88): p. 47313-47318.
24. Jayakumarai, G., et al., *Phytofabrication and characterization of monodisperse copper oxide nanoparticles using Albizia lebbeck leaf extract.* Applied Nanoscience, 2015. **5**(8): p. 1017-1021.

25. Sathiyavimal, S., et al., *Biogenesis of copper oxide nanoparticles (CuONPs) using Sida acuta and their incorporation over cotton fabrics to prevent the pathogenicity of Gram negative and Gram positive bacteria.* Journal of Photochemistry and Photobiology B: Biology, 2018. **188**: p. 126-134.
26. Diallo, A., et al., *Green synthesis of Co3O4 nanoparticles via Aspalathus linearis: physical properties.* Green Chemistry Letters and Reviews, 2015. **8**(3-4): p. 30-36.
27. Bibi, I., et al., *Corrigendum to 'green and eco-friendly synthesis of cobalt-oxide nanoparticle: characterization and photo-catalytic activity'[Adv. Powder Technol. 28 (2017) 2035–2043].* Advanced Powder Technology, 2017. **10**(28): p. 2796.
28. Lee, R.B., et al., *The relationship between iron and Ilmenite for photocatalyst degradation.* Advanced Powder Technology, 2018. **29**(8): p. 1779-1786.
29. Rehman, S., A. Mumtaz, and S. Hasanain, *Size effects on the magnetic and optical properties of CuO nanoparticles.* Journal of Nanoparticle Research, 2011. **13**(6): p. 2497-2507.
30. Neeleshwar, S., et al., *Size-dependent properties of CdSe quantum dots.* Physical Review B, 2005. **71**(20): p. 201307.
31. Huang, X., et al., *Plasmonic photothermal therapy (PPTT) using gold nanoparticles.* Lasers in medical science, 2008. **23**(3): p. 217.
32. Vilchis-Nestor, A.R., et al., *Solventless synthesis and optical properties of Au and Ag nanoparticles using Camellia sinensis extract.* Materials letters, 2008. **62**(17-18): p. 3103-3105.
33. Nazeruddin, G., et al., *In-vitro bio-fabrication of silver nanoparticle using Trigonella foenum seed extract.* Research Journal of Pharmaceutical, Biological and Chemical Sciences, 2014. **5**(2): p. 167-175.